Author(s): M J Prest, Y Wang, F Huang and M J Lancaster
Article Title: Tuning of a superconducting microwave resonator at 77 K using an integrated micromachined silicon vertical actuator
Year of publication: 2010
Link to published article:
http://dx.doi.org/10.1088/0960-1317/20/9/095032

Tuning of a Superconducting Microwave Resonator at 77 K using an Integrated Micromachined Silicon Vertical Actuator

M J Prest[1], Y Wang[2], F Huang[2] and M J Lancaster[2,3]

[1]Department of Physics, University of Warwick, CV4 7AL, UK.
[2]School of Electronic, Electrical and Computer Engineering, University of Birmingham, B15 2TT, UK

[3]Email: m.j.lancaster@bham.ac.uk

Abstract. A silicon micromachined actuator is used to tune a high temperature superconducting microwave resonator. The superconducting resonator is only 1.24 mm by 0.66 mm and demonstrates a Q of up to 1078 at 6.3 GHz and at 77 K. A tuning range of 12% is demonstrated with a maximum applied voltage of 40 V. The frequency of the resonator is controlled by the proximity of a silicon tuning probe. The room temperature resistivity of the silicon is measured to be 20 Ω cm; this value drops as the device is cooled, but remains the limiting factor in the quality factor of the device. This proof of principle experiment demonstrates the application of silicon micromachining for tuning of superconducting microwave circuits; which is achieved despite the difficulties presented by differing material properties and thermal constraints when cooling to 77 K.

Keywords. superconductivity, MEMS, YBCO, MgO, semiconductor, flip-chip

1. Introduction

There has been increasing interest in tunable microwave circuits in recent years. We present here a novel method to tune superconducting microwave circuits using a silicon micromachined actuator.

Superconducting microwave resonators have a high Q because of their extremely low surface resistance at microwave frequencies in the low gigahertz region. High temperature superconductors (HTS) allow operation at a temperature of 77 K where cooling is easily achieved using liquid nitrogen. We use Yttrium Barium Copper Oxide (YBCO) as the HTS material, which is grown on a Magnesium Oxide (MgO) substrate. The microwave structures are of a microstrip design, which employs YBCO layers on both sides of the 0.5 mm thick MgO wafer. The top YBCO layer is patterned by ion beam milling to form the circuit elements. The backside YBCO layer is not patterned and forms a ground plane.

Electrostatic actuators such as the one described in this work are popular because of their low power dissipation. Electrostatic switches for RF applications are often fabricated from thin films of metal, semiconductors and dielectrics. Such thin films often suffer from fabrication induced stress and dielectric charging during operation. Our device employs a thicker layer (45 μm) of crystalline silicon as the moving part and an “air-gap” as the dielectric. We particularly wanted to avoid stress related problems as our device is subject to large temperature changes (fabrication above room temperature and operation at 77 K). We use a silicon on insulator (SOI) wafer as our starting material; these are commonly available and consist of two silicon layers (in our case 45 μm and 350 μm thickness) bonded together with a silicon dioxide layer (1 μm thickness) in between. The moving parts are released by first etching the silicon, then the silicon dioxide.

This work aims to develop a hybrid technology that uses the advantages of both micromachined tuning and the high Q of a superconducting resonator. We use standard silicon MEMS processing and standard HTS thin film processing, with a flip-chip bonding step to combine the two technologies. Our device enables a continuously variable adjustment of frequency. The ultimate objective of our work is to develop tunable filters and other components based on these hybrid structures.

We have previously demonstrated this hybrid technology using a silicon comb-drive horizontal actuator [1]. In the present work we demonstrate an alternative actuator with improved tuning range and reliability. Also, in common with our previous work, we use compliant support springs and a stress-buffering frame to isolate the actuator from thermally induced stress when cooling to low temperatures. The thermal stress arises from differences in thermal expansion coefficients between the MgO substrate (supporting the HTS) and the silicon.

There are several other groups with an interest in tuning of superconducting RF circuits [2]-[6]. In 2003 Hijazi *et al.* demonstrated a superconducting RF micro-electro-mechanical switch using an electrostatically actuated, thin film gold membrane [3]. In 2005 Prophet *et al.* also demonstrated a gold film membrane switch with multiple fixed frequencies [4]. Previous work [3]-[6], including work initiated at Birmingham [5], concentrated on thin film actuators and this is the first reported work on vertical tuners based on SOI wafers.

The design of our silicon actuator is based on the work of Hah, Yoon and Hong [7] and we have used their operation principle and design calculations in this work. They used a push-pull actuator with torsion springs as an on-off switch for signals between 500 MHz and 4 GHz and their device operated at room temperature. The main structural layer in their case was gold and the total thickness of their movable structure was 1.4 µm. In our case the structural layer is silicon and the thickness is 45 µm. Our actuator is not used as an on-off switch; instead it allows continuous tuning of a microwave resonator by adjusting the angle of rotation and therefore the vertical height of a tuning probe.

2. Tuning principle

The HTS resonator consists of an interdigital capacitor and an inductor (as shown in figure 1); the structure resonates at approximately 6 GHz [8]. The tuning probe is fabricated from low resistivity silicon (~ 20 Ωcm at room temperature) and lies directly above the HTS capacitor as shown in figure 2. A cross section is shown in figure 3. The actuator voltage controls the probe height above the capacitor fingers. The vertical gap between the HTS resonator and the tuning probe with zero actuator bias is nominally 6.6 µm, set by a photo resist spacer. As shown in figure 4, the silicon actuator is suspended by a torsion spring, electrostatic actuation pads either side of the spring cause the spring to be twisted one way or the other. An arm extends out from the cradle of the actuator so that a silicon probe at the end is suspended above the microwave resonator.

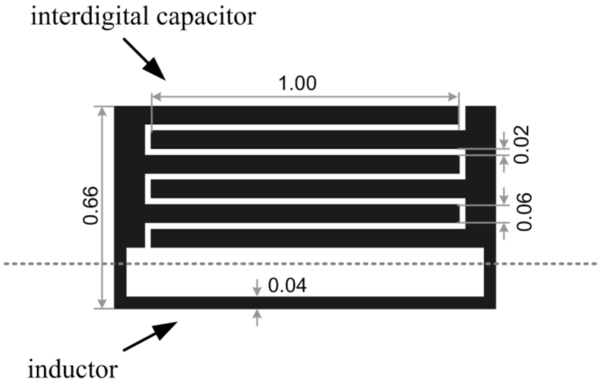

Fig. 1. HTS resonator close-up showing interdigital capacitor (above dotted line) and inductor (below dotted line). Dimensions are in mm. The total width of the resonator is 1.24 mm. From [1].

The gap between the silicon tuning probe and the resonator can be adjusted and held at any value between 0 and 15 µm by adjusting the applied dc bias, and hence the tilt angle of the actuator cradle. The long length of the probe arm (~ 2.6 mm) ensures that movement at the actuation end does not exceed the point at which the electrostatic force is greater than the returning spring force (the pull-in condition). The actuator design used calculations described by Hah, Yoon and Hong [7] and further details of a similar silicon actuator fabrication process were given in our previous publication [1]. Calculation parameters for our actuator are summarised in table 1.

A plot of height versus actuator voltage is shown in figure 5. The plot shows that the probe should be fully pulled down for an applied bias of 40 V, however, there are uncertainties in the calculations, particularly the shear modulus of silicon, for which we have used a room temperature value. The Young's modulus of silicon is fairly constant between room temperature and 77 K [8], so we have assumed that there is also little variation in the shear modulus. The initial height was measured by breaking the device apart after the measurement and measuring the thickness of the photo-resist spacer.

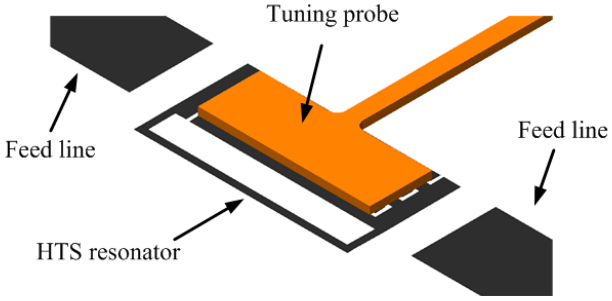

Fig. 2. Close-up of the tuning probe. It is difficult to see the initial gap between the tuning probe and HTS resonator of 6.6 µm in this figure, because the dimensions of the probe (1000 µm × 360 µm) are much greater than the gap.

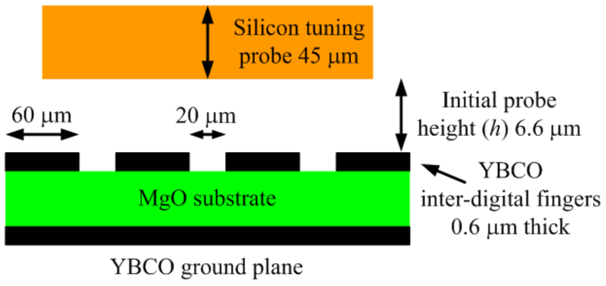

Fig. 3. A cross-section of the silicon tuning probe and HTS resonator as used for the simulations. The diagram shows probe height (h), which is adjusted by the micromachined actuator to tune the resonator. Not drawn to scale.

Table 1. Parameters for probe height calculations as described in Hah, Yoon and Hong [7]. There is no insulator in our device, therefore the insulator thickness (t_d) from equation 2 in [7] is omitted from the table below.

Parameter	Value
Shear modulus of silicon (G)	80 GPa
Spring width (w_s)	50 µm
Spring height (t_s)	45 µm
Spring length (l_s)	1500 µm
Top electrode width (w_{te})	3500 µm
Top electrode length (l_{te})	750 µm
Bottom electrode length (w_{be})	750 µm
Initial height (h_0)	6.6 µm

The structure has been simulated, using the commercial software package Sonnet [9], to determine the change in resonant frequency as a function of probe height. When the silicon tuning probe is lowered, the additional volume of dielectric close to the capacitor causes an increase in capacitance and a consequent reduction in frequency. The simulated frequency change as a function of the silicon height is shown in figure 6. It shows that the frequency of the resonator varies from 6.394 GHz for height 15 μm to 5.156 GHz for height 1 μm, a 19.4% range (defined by frequency variation as a fraction of the maximum frequency). The frequency variation is dependent upon the permittivity of the silicon (a value of 11.9 has been used in the simulations). The tuning range is greater than that of our previously reported horizontal tuner [1], which had a simulated variation from 6.075 GHz to 5.699 GHz (6.2%) and a measured variation of 4.6% with a 40 μm horizontal movement. The quality factor of the horizontal tuner was about 300 and almost independent of resonator frequency.

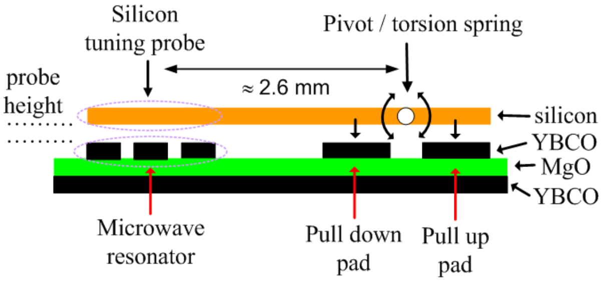

Fig. 4. A cross-section of the actuator and tuning probe showing how the probe height is adjusted. Probe height is initially 6.6 μm. Bias applied between the actuator and pull up pad produces an attraction force to the right of the pivot, so that the probe tip moves up. Bias applied between the actuator and the pull down pad, to the left of the pivot, causes the probe tip to move down.

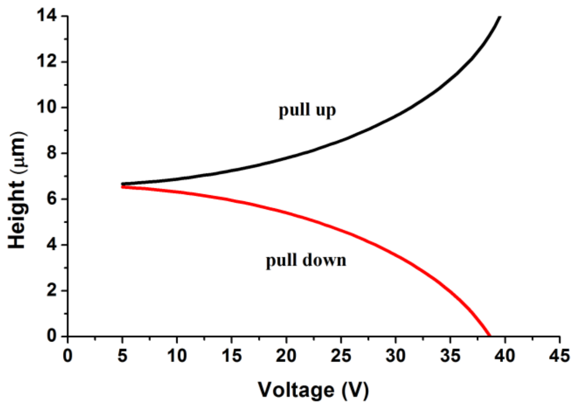

Fig. 5. Calculated height of tuning probe versus applied bias using parameters in table 1.

The losses contributing to the overall resonator Q come mainly from the losses in the silicon. Without the silicon actuator the quality factor of the resonator has been measured to be 2286. This corresponds to an unloaded Q of 4531. This value is not as high as many superconducting resonators reported in the literature because the size of the circuit is extremely small. Simulations show the loaded Q associated with the silicon tuner, the YBCO resonator and the MgO substrate to vary from 1254 to 44 as the height of the tuner changes from 15 μm to 1 μm. A graph of this variation is shown in figure 7. The resistivity of the silicon was set to 430 Ωcm (from the nominal 20 Ωcm at room temperature), in order to fit a measured loaded quality factor of 493 at the “rest” position. This increase of the resistivity is quite reasonable considering that the device operates at 77 K; silicon resistivity rises as the temperature is reduced because of the reduced carrier concentration at low temperatures. It should also be noted that these values of loaded Q could be improved either by fabricating the device from higher resistivity material (lower doped or intrinsic silicon) or increasing the resistivity by further reduction of the operation temperature.

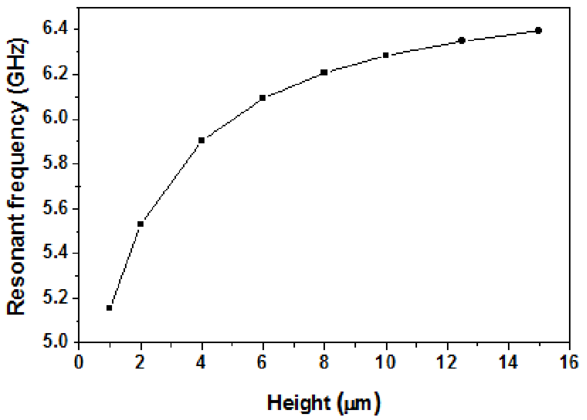

Fig. 6. Simulated tuning range. The dimensions used for the interdigital capacitor are shown in figure 1 and the dimensions of the tuning probe are given in figures 2 and 3.

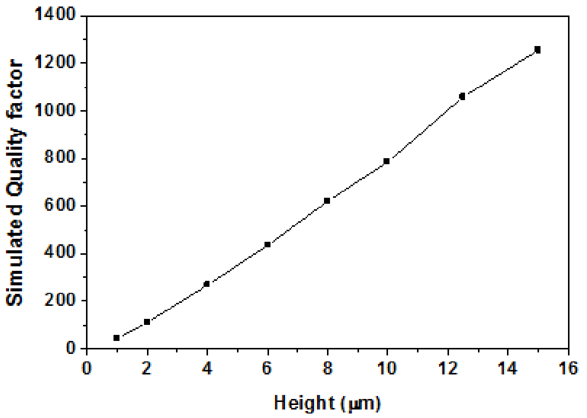

Fig. 7. Simulated loaded quality factor of the resonator. The dimensions used for the interdigital capacitor are shown in figure 1 and the dimensions of the tuning probe are given in figures 2 and 3. The superconductor has a surface sheet resistance of 1.49×10^{-4} Ω/□, the silicon has a resistivity of 430 Ω·cm, and the MgO has a loss tangent of 6.2×10^{-6}.

3. Fabrication

HTS resonator was fabricated from yttrium barium copper oxide (YBCO) on a magnesium oxide (MgO) substrate, as described in section 1.

The layout of the full HTS part of the circuit is shown in figure 8. The figure shows the resonator together with the feed lines and narrow coupling gaps. The microstrip feed lines were designed to allow coplanar probes to contact the circuit for measurements. A microstrip radial stub was used to match the coplanar input to the microstrip [10]. The structure at the top of figure 8 is where the MEMS actuator was attached (by flip-chip bonding) and shows where the dc tuning voltage was applied. Only the large (1.2 mm x 1.2 mm) square pads at either side of the actuator were electrically bonded to the actuator (using silver epoxy). The pull up and pull down pads attract the actuator electrostatically. There was a 6.6 μm spacer between the inner frame of the actuator and the HTS layer, this spacer was fabricated from 6.4 μm of photo-resist and 0.2 μm of gold.

The coefficients of thermal expansion of silicon and MgO differ by approximately a factor of four at room temperature; 2.5×10^{-6} K^{-1} for silicon [11] and 11×10^{-6} K^{-1} for MgO [12]. Because of this large difference in expansion coefficients and the high Young's modulus of the materials, differential expansion and contraction would cause large forces during thermal cycling between room temperature and 77 K. We therefore employed compliant support springs as introduced in our previous publication [1].

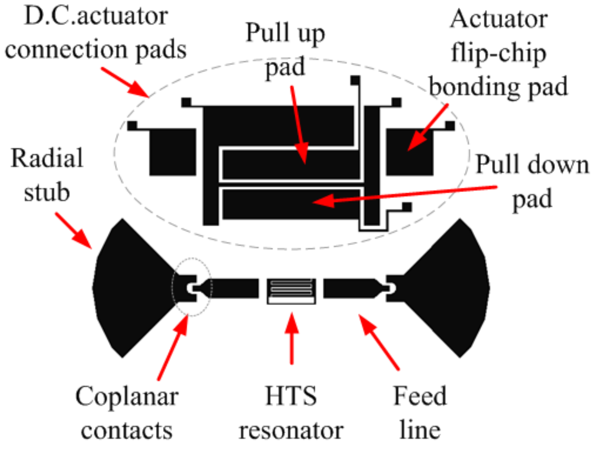

Fig. 8. Layout of HTS circuit. Showing 90 degree radial stub, microstrip to coplanar transitions and pads for the actuator. The actuator only requires 3 bias pads to provide full movement. The two bonding pads connect electrically to the actuator silicon and are common to both the pull up and pull down connections. When pads were not required for actuation, they were left unbiased (floating potential).

Figure 9 shows a close-up of the compliant support springs, and figure 10 shows the operation principle. As the device is cooled to low temperature the MgO substrate will contract faster than the silicon. The differential thermal contraction will compress the compliant support springs which are linked together by the inner support frame of the actuator. The inner support frame is much stiffer than the support springs, so it will not be significantly deformed, and therefore the stress applied to the torsion springs of the actuator will be negligible. In other words the inner frame provides stress-buffering, it prevents stress from being applied to the torsion springs. A slight deformation of the compliant support springs was observed in the measured device at 77 K. Figure 11 shows the full device, as used in this paper.

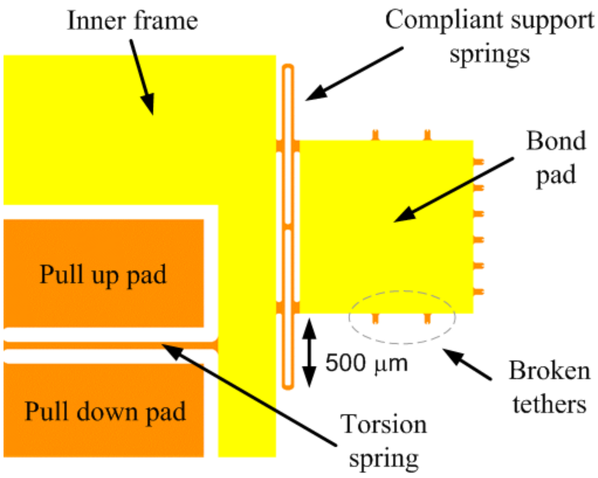

Fig. 9. A close-up of the compliant support springs. Each of the spring beams is 500 μm long by 20 μm wide by 45 μm high. Also shown is the bond pad after attachment to the RF substrate (with broken tethers around the edge – there is a silicon frame around the device before flip-chip bonding to the substrate, this frame is broken away after bonding leaving the broken tethers, further details are given in [1]). The bond pads are 1.2 mm × 1.2 mm square.

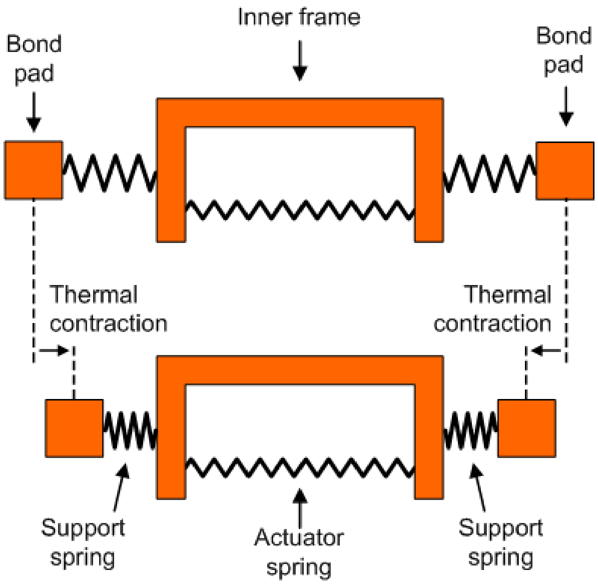

Fig. 10. The inner support frame is much more rigid than the support springs, so when thermal contraction occurs, whilst cooling to 77 K, only the support springs are compressed. The delicate actuator spring is virtually unaffected by the thermal compression.

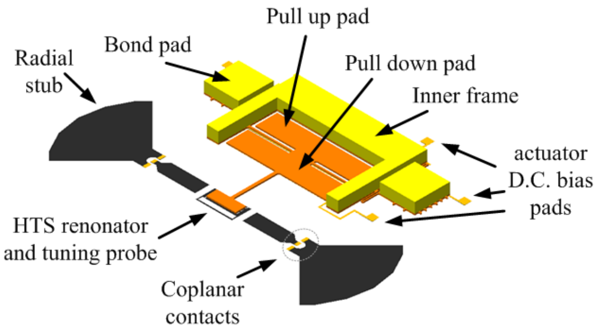

Fig. 11. The full device showing the HTS circuit with silicon actuator for tuning. The total size of this device fits comfortably within a 1 cm x 1 cm square. There is about 6 mm between the centres of the actuator bond pads.

4. Measurements and Results

The device was cooled to 77 K using a Desert Scientific cryogenic probe station. The actuator was biased using a Keithley 237 voltage source and the S-parameters were measured using an Agilent 8722ES network analyser. Low-temperature line-reflect-reflect-match on-wafer calibrations were performed at 77 K. The analyzer source power was set at -10 dBm. It was important to measure the device with no incident light, otherwise photon generated charge carriers would have reduced the silicon resistivity.

Figure 12 shows that as the actuation voltage was varied, the tuning probe moved causing the centre frequency of the resonator to shift. The measured tuning range is about 12%.

The measured resonator centre frequencies and quality factors are shown together with the simulation results in figure 13 (using the calculated heights from figure 5). It is clear that the loaded quality factor drops off as the tuning actuator is pulled down towards the HTS resonator; this is to be expected and is a result of dielectric loss in the silicon. This dielectric loss could be reduced by using higher resistivity silicon. Measurement and simulation results are also compared in table 2. There is good agreement between the simulation and measurement results. The measured tuning range is a little narrower than predicted by the simulations, and the measured quality factors agree reasonably well with the simulated values. The simulation is a simplified model which assumes that the tuning probe remains parallel to the resonator as the height changes; in reality there is a slight tilting of the tuning probe, this may contribute to the small discrepancies.

5. Conclusions

We have demonstrated a tunable HTS microwave resonator with a measured tuning range of 12%. The loaded quality factor varies from 1078 at the highest frequency (6.30 GHz) to 104 at the lowest frequency (5.54 GHz). This large variation in quality factor is a result of the variation in vertical gap between the silicon tuning probe and the HTS resonator. In the future we hope to reduce the operating temperature and hence increase the silicon resistivity. However, we may reach a point at which the high silicon resistivity begins to affect the biasing and hence the movement of the silicon actuator. As an alternative it may be possible to replace just the end of the tuning probe with a high resistivity material such as sapphire. More complex tunable circuits such as filters are being considered using this hybrid technology.

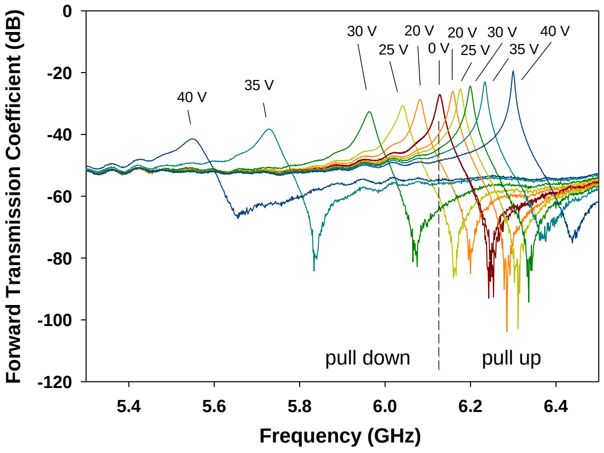

Fig. 12. Forward transmission coefficient (S-parameter S21), measurements for resonator at 77 K, showing tuning of peak frequency with varying actuator bias.

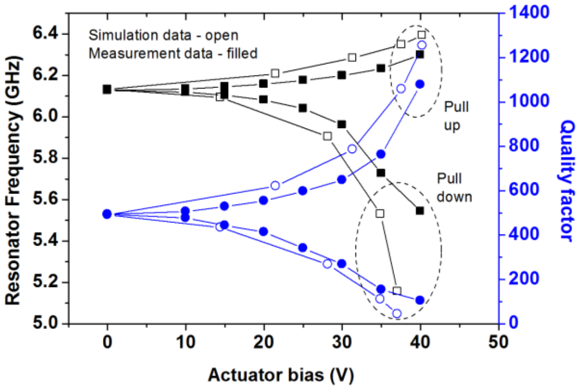

Fig. 13. Measurements of resonant frequency and loaded quality factor versus actuator bias. Simulated frequency (open squares), measured frequency (closed squares), simulated quality factor (open circles), measured quality factor (closed circles).

Table 2. Comparison between the simulated and measured frequency and loaded quality factor at 77 K.

Height (µm)	Actuator bias	Simulated		Measured	
		f_0 (GHz)	Q	f_0 (GHz)	Q
2	35 V (Pull down)	5.53	111	5.73	154
6.6	0 V (Rest)	6.13	494	6.13	494
15	40 V (Pull up)	6.39	1254	6.30	1078

Acknowledgments

The silicon rocking actuator structure was fabricated using facilities at the MC2 clean room at Chalmers University of Technology in Göteborg, Sweden. The access to this facility was funded by a Framework 6 European grant: 'Research Infrastructures Action'. The authors thank the staff of the nanofabrication laboratory at Chalmers University, particularly Ulf Södervall, Johan Andersson and Göran Petersson, for their support, advice and assistance with the silicon MEMS processing. Additional funding was provided by the Engineering and Physical Sciences Research Council, UK.

References

[1] Prest M J, Wang Y, Huang F and Lancaster M J 2008 Silicon comb-drive actuators for low-temperature tuning of superconducting microwave circuits *J. Micromech. Microeng.* **18** 125003-125009

[2] Tsuzuki G, Hernandez M P and Willemsen B A 2005 Tuning fork filter design for hand scribe tuning *Microwave Symp. Dig. 2005 IEEE MTT-S International*

[3] Hijazi Y S, Hanna D, Fairweather D, Vlasov Y A and Larkins G L 2003 Fabrication of a superconducting MEM shunt switch for RF applications *IEEE Trans. on Appl. Superconductivity* **13** 700-703.

[4] Prophet E M, Musolf J, Zuck B F, Jimenez S, Kihlstrom K E, Willemsen B A 2005 Highly-Selective Electronically-Tunable Cryogenic Filters Using Monolithic, Discretely-Switchable MEMS Capacitor Arrays IEEE Transactions on Applied Superconductivity 15 956-959

[5] Su H T, Llamas-Garro I., Lancaster M J, Prest M, Park J-H, Kim J-M, Baek C-W and Kim Y-K 2006 Performance of RF MEMS switches at low temperatures Electronics Letters 42 1219-1220

[6] Abbaspour-Tamijani A, Dussopt L, and Rebeiz G M 2003 Miniature and tunable filters using MEMS capacitors *IEEE Trans. MTT* **51** 1878-1885

[7] Hah D, Yoon E and Hong S 2000 A low-voltage actuated micromachined microwave switch using torsion springs and leverage *IEEE Trans. MTT* **48** 2540

[8] Prest M J, Wang Y, Huang F and Lancaster M J 2008 Silicon MEMS tunable supeconducting microwave circuits *Proc. 9th Int. Symp. on RF MEMS and RF Microsystems* (MEMSWAVE 2008) (Heraklion, Greece, 1-3 July 2008)

[9] Sonnet Simulation Tools 2006 Sonnet Software Inc., (Syracuse, NY)

[10] Wang Y, Lancaster M J 2007 Coplanar to Microstrip Transitions for on-wafer Measurements *Microwave and Optical Technology Letters* **49** 100-103

[11] White M J 1973 Thermal expansion of reference materials: copper, silica and silicon *J. Phys. D: Appl. Phys.* **6** 2070

[12] Smith D K and Leider H R 1968 Low-temperature thermal expansion of LiH, MgO and CaO *J. Appl. Cryst.* **1** 246